

Two new Bodipy-carbazole derivatives as metal-free photosensitizers in photocatalytic oxidation of 1,5-dihydroxynaphthalene

Yuanming Li^a, Yaxiong Wei^{b,*}, Xiaoguo Zhou^{a,*}

^a Department of Chemical Physics, University of Science and Technology of China, Hefei, 230026, China

^b Shenzhen Key Laboratory of Polymer Science and Technology, College of Materials Science and Engineering, Shenzhen University, Shenzhen, 518060, China

ARTICLE INFO

Keywords:

Organic photosensitizer
Triplet photosensitizer
Photo-oxidation
Solvent effect
Intersystem crossing

ABSTRACT

Two new metal-free photosensitizers of Bodipy-carbazole derivatives, Phenyl-Bodipy-Carbazole (BC) and Carbazole-Bodipy-Carbazole (CBC), were synthesized. The transient absorption spectroscopy and the density functional theory calculations verify that the triplet Bodipy unit is produced in the dyads via an intramolecular charge transfer in the Franck-Condon excitation. Moreover, an apparent dependence on the solvent polarity was observed for these triplet states lifetimes, e.g. 9.6 and 118.2 μs in cyclohexane, while, 204.7 and 464.7 μs in dichloroethane for BC and CBC, respectively, as well as the triplet state quantum yields. With the increase of solvent polarity, the prolonged lifetime and the decreased quantum yield of the triplet BC and CBC convince us the charge-transfer mechanism for ISC process. In addition, the photo-oxidation rate constants of 1,5-dihydroxynaphthalene with these triplet photosensitizers are determined to be $1.11 \times 10^{-3} \text{ min}^{-1}$ and $2.54 \times 10^{-3} \text{ min}^{-1}$ for BC and CBC, respectively.

1. Introduction

Triplet photosensitizers have been extensively applied in many fields, such as photocatalysis organic reactions [1–4], photodynamic therapy [5,6], and triplet-triplet annihilation upconversion [7–9]. During the past decades, many types of triplet photosensitizers were developed, however, most of which were the transition metal complexes, such as, Ru(bpy)₃Cl₂ [10], Pt(II) porphyrin [11–13], Pd(II) porphyrin [14,15], cyclometalated Ir(III) [16] and Os(II) 110-Phenanthroline [17,18]. It is easily comprehended that the heavy-metal-atom effect can facilitate intersystem crossing (ISC) to yield the corresponding triplet state upon photoexcitation [19]. However, considering their disadvantages of expensive costs and usually weak absorption in the visible range [20], developing cheap and environmentally friendly metal-free photosensitizers is still ongoing.

In past decades, some organic triplet photosensitizers were synthesized as the representative metal-free ones, with the highly efficient intersystem crossing (ISC) and the strong absorption in the visible range, e.g. 2,3-butanedione and benzophenone [21–23]. Briefly, they can be classified into three families, i.e., one with the (n, π*) → (π, π*) transition, the second with a small energy gap of S₁/T_n states, and the fullerene derivatives like C₆₀ and C₇₀ [7,24]. Very recently, Zhao et al., have reported a special ISC mechanism so-called the spin-orbit charge transfer enhanced ISC (SOCT-ISC) [25,26]. This novel SOCT-ISC process occurs due to a twist angle between the electron donor and receptor units in a dyad molecule [25]. Thus, it gives

us an additional motivation to clarify the role of electron transfer (or charge transfer) in new synthesized triplet photosensitizers.

In this work, two new Bodipy (BDP) derivatives, Phenyl-Bodipy-Carbazole (BC) and Carbazole-Bodipy-Carbazole (CBC), were designed (Scheme 1) and synthesized. In these molecules, the BDP unit plays a strong light-harvester role in the visible range, while the carbazole unit is connected to BDP with a carbon-carbon triple bond, expanding the π-conjugated structure. Although the similar molecular structures have been reported [7,27], the photophysical properties of BC and CBC as triplet photosensitizers are not studied. Herein, the steady-state and nanosecond time-resolved transient absorption spectroscopy has been performed for BC and CBC in different solvents to obtain their triplet lifetimes. With the aid of density functional theory (DFT) calculations, the electrochemical characterization reveals the charge transfer involved in Franck-Condon excitation, which is believed as the crucial factor to improve ISC efficiencies of BC and CBC. The solvent effect is further discussed in the title systems, to provide more clues for this mechanism. Moreover, when using them in photocatalytic oxidation of 1,5-dihydroxynaphthalene (DHN), the kinetic measurements provide us the related reaction rates.

2. Experimental and computational sections

All the precursors of analytical reagent were purchased from Aladdin Inc. and were directly used in experiments without any

* Corresponding authors.

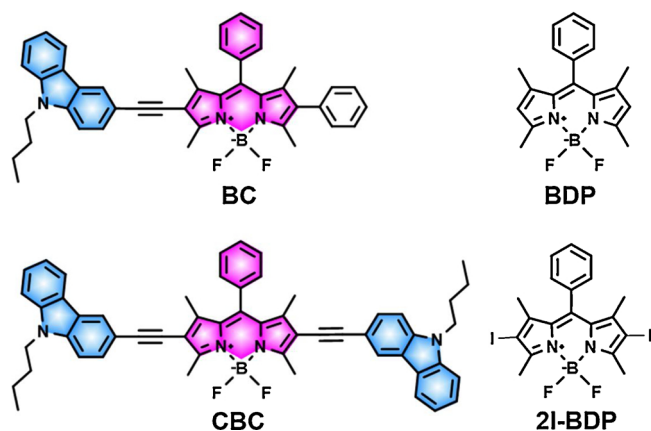
E-mail addresses: davidl@mail.ustc.edu.cn (Y. Wei), xzhou@ustc.edu.cn (X. Zhou).

<https://doi.org/10.1016/j.jphotochem.2020.112713>

Received 19 February 2020; Received in revised form 8 June 2020; Accepted 14 June 2020

Available online 16 June 2020

1010-6030/ © 2020 Elsevier B.V. All rights reserved.



Scheme 1. Molecular structures of Bodipy and its derivatives, i.e. BC, CBC, BDP monomer, and diiodo-Bodipy (2I-BDP).

purification. BC and CBC were synthesized along the route and were characterized with ^1H NMR spectra as described in Fig. S1-S3 of ESI. The mother liquors of the synthesized samples were prepared in toluene with the concentration of 1×10^{-3} M, then were diluted to the concentration of 1×10^{-5} M in different solvents, such as cyclohexane, toluene, dichloroethane, respectively, for spectroscopic measurements.

^1H NMR spectra were measured with a 400 MHz spectrophotometer (AVANCE III 400, Bruker), where CDCl_3 was used as solvent and TMS was the standard for which $\delta = 0.00$ ppm. High-resolution mass spectra were measured with a spectrometer (GCT, Micromass UK). UV-vis absorption spectra were recorded in the wavelength range of 300–800 nm with a spectrophotometer (UV-3600, Shimadzu). The steady-state fluorescence emission was measured with a spectrophotometer (F-4600, Shimadzu) in the range of 400–800 nm.

The nanosecond time-resolved transient absorption spectra were measured with a home-built laser flash photolysis system [17,24]. The second harmonic (532 nm) of a Q-Switched Nd: YAG laser (PRO-190, Spectra Physics) was used as the excitation source (pulse duration 8 ns, repetition rate of 10 Hz, pulse energy < 10 mJ/pulse). A 500 W Xenon lamp (71PX5002) was used as the analyzing light, and passed through a quartz cuvette (10×10 mm) perpendicularly with the pulsed laser. The optical absorption path length was 10 mm. A monochromator (Omni- λ 5025) equipped with a photomultiplier (CR131, Hamamatsu) was used to record the transient absorption spectra within a wavelength range of 300–800 nm. The typical spectral resolution was less than 1 nm. The fluorescence quantum yield and the triplet quantum yield were calculated as indicated in ESI.

Cyclic voltammograms were recorded at room temperature after purging with Ar for 30 min. A three-electrode electrolytic cell was used,

with 0.1 M tetrabutylammonium hexafluorophosphate ($\text{Bu}_4\text{N}[\text{PF}_6]$) as the supporting electrolyte, a glassy carbon electrode as the working electrode, and a platinum electrode as the counter electrode. A non-aqueous Ag/AgNO_3 (0.1 M in acetonitrile) reference electrode was contained in a separate compartment connected to the solution via semipermeable membrane. DCM was used as the solvent, scan-rate of 50 mV/s, and ferrocene was added as the internal reference.

In photocatalytic oxidation experiments, a 30 mL reagent bottle was set on a magnetic stirrer, and a rectangular parallelepiped glass jar containing 50 g/L sodium nitrite solution (filtering out ultraviolet light having a short wavelength of 385 nm and long-wavelength infrared light) was placed between a xenon lamp (300 W) and the reagent bottle. A careful adjustment was done to ensure that the light source, glass jar and reagent bottle are in a straight line, making the evenly distributed light on the reagent bottle surface. The optical power density was kept at $40 \text{ mW}/\text{cm}^2$ by adjusting the relative distance. The mixed solvent of dichloromethane/methanol (9:1, V/V) was added to the reagent bottle, with 1,5-dihydroxynaphthalene (DHN) (1×10^{-4} M) and photosensitizers (1×10^{-5} M). The UV-vis absorption spectra of the mixed solutions were measured with the light on or off every seven minutes. The production of Juglone as the oxidation product was detected by measuring the increase of the absorption intensity at 427 nm [8].

Geometries of the compounds were optimized using density functional theory (DFT) with B3LYP function and 6–31 G(d) basis set. The vibrational frequency analyses were performed to verify the true minima for the optimized structures. Then the spin density surfaces of the dyads and the energy gaps between the ground state and the triplet excited state were calculated at the same level of theory. The vertical excitation energies were directly compared with the experimental absorption spectra, and the spectral assignments were obtained subsequently. The PCM model was applied to evaluate the solvent effect. All these calculations were carried out with the Gaussian 09 W program package [7,28].

3. Results and discussions

3.1. UV-vis absorption and fluorescence emission spectra

Fig. 1a and b shows the steady-state absorption spectra of BC and CBC in different solvents with solid lines. In cyclohexane, BC has a strong absorption peak at 553 nm ($\epsilon = 4.46 \times 10^4 \text{ M}^{-1} \text{ cm}^{-1}$), while CBC has an intense absorption centered at 599 nm ($\epsilon = 3.28 \times 10^4 \text{ M}^{-1} \text{ cm}^{-1}$), both of which can be easily assigned to the $^1\pi\pi^*$ states. Compared to the BDP monomer which absorption peak is located at 517 nm [7], both BC and CBC show the red-shifts of 26 and 82 nm, respectively. Evidently, the red-shifts are due to the expansion of π -conjugated structure by the carbon-carbon triple bond connecting the carbazole and BDP units. The reduction of the π -electron delocalization

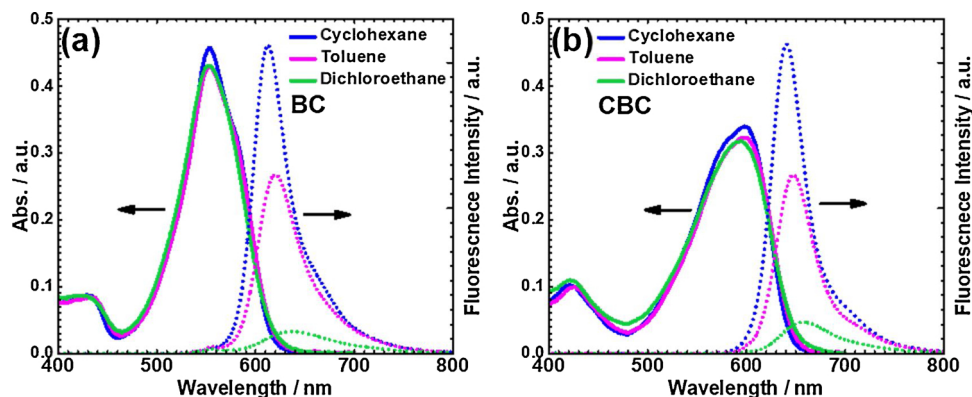


Fig. 1. The UV-vis absorption (solid lines) and fluorescence emission (dot lines) spectra (25 °C) of BC (a) and CBC (b) in cyclohexane, toluene, dichloroethane, respectively, where the concentrations are 1×10^{-5} M.

energy implies the electronic coupling between the carbazole and BDP units. Moreover, as shown in Fig. 1a, a blue-shift of 5 nm exists for the absorption peak of BC in dichloroethane in comparison with cyclohexane, and the absorption intensity almost remains. The similar results were observed for CBC with a blue-shift of 8 nm. Although the polarity of solvents is well-known to be able to influence the excitation energy of $^1\pi\pi^*$ state [29], it is not significant for the Franck-Condon excitation of BC and CBC.

To our surprise, the fluorescence emission intensity of BC is dramatically decreased with the increase of solvent polarity as shown in Fig. 1a. The fluorescence quantum yield (Φ_F) is determined to be 16 % in cyclohexane, but 2.3 % in dichloroethane, using the fluorescence of 2I-BDP as the standard ($\Phi_{std} = 2.7$ % in ACN). The calculation details are described in the ESI. Meanwhile, the emission peak exhibits a red-shift from 610 nm in cyclohexane to 630 nm in dichloroethane. A similar solvent-polarity-dependent behavior was observed for CBC too, as indicated in Fig. 1b and Table 1. From the red shift of the fluorescence peak position, we can draw a conclusion that the molecular dipole moment in the ground state (μ_g) is smaller than that of the excited state (μ_e) [30]. In this case of $\mu_g < \mu_e$, the excited state is stabilized more markedly, reducing the energy gap. Moreover, it is worth noting that the fluorescence emission of the BDP monomer shows no dependence on solvent polarity [26].

In order to achieve the reliable spectral assignments, the frontier molecular orbitals and the corresponding excitation energies of BC and CBC were calculated at the DFT level of theory. The oscillator strengths (f) of the major Franck-Condon transitions were calculated as the same level and to directly compare with the experimental spectra. Fig. 2 shows the calculated data of CBC as a representative, as well as the comparisons of the experimental and calculated spectra of BC and CBC.

The optimized geometries of BC and CBC in the ground state were summarized in the ESI. In both BDP derivatives, the BDP core and the carbazole unit take a coplanar configuration, which is apparently different from the necessary twist geometry in SOCT-ISC process [25]. Thus, the SOCT-ISC mechanism is impossible for these two BDP derivatives. Moreover, this skeleton planar geometry makes the electronic coupling of the BDP and carbazole units feasible to occur, which can be verified by the red-shift of the absorption peaks. Moreover, as shown in Fig. 2a, the highest occupied molecular orbital (HOMO) of BC and CBC is contributed by both the BDP and carbazole units, while the lowest unoccupied molecular orbital (LUMO) is mainly located only at the BDP unit. Therefore, the intramolecular charge transfer inevitably occurs during the Franck-Condon excitation. In addition, as indicated in Fig. 2b and c, the calculated excitation energies of the Franck-Condon transitions for BC and CBC are generally consistent with their absorption spectra. CBC shows a slight red shift in the transition of HOMO \rightarrow

LUMO compared to BC indeed. Of special interests is that the spin density of the lowest triplet state (T_1) is localized at the BDP and partial carbazole units in BC and CBC (Fig. S7). Thus, the triplet state in the BC and CBC dyads might be produced via the intramolecular charge transfer and recombination.

3.2. Cyclic voltammogram

To evaluate the possibility of intermolecular charge transfer in Bodipy derivatives, cyclic voltammograms (CVs) were applied to obtain their redox potentials. Fig. 3 shows the recorded cyclic voltammograms of BDP monomer and BC. For BDP monomer, a reversible oxidation wave at +1.12 V and a reversible reduction wave at -1.14 V were observed, which are basically consistent with the reported data [26]. However, only one reversible oxidation wave was observed at +0.93 V for BC, while the oxidation wave of carbazole unit did not exist in Fig. 3. This evidently indicates a strong coupling between the carbazole and BDP units in the BC dyad due to being connected by a carbon-carbon triple bond, which is also consistent with the above conclusion of absorption spectroscopy. Moreover, the reduction wave of BC was located at -1.22 V. Such a small change from that of BDP implies that the charge density in the ground state is mainly distributed in both the BDP and carbazole units, while the charge density in the excited state is only distributed in the BDP unit. Thus, an intramolecular charge transfer could feasibly occur from the carbazole unit to the BDP moiety during the Franck-Condon excitation.

3.3. Nanosecond transient absorption spectra

Fig. 4a-c show the nanosecond transient absorption spectra of BC in the deoxygenated cyclohexane, toluene, and dichloroethane, respectively. Upon the photoexcitation at 532 nm, the strong ground-state bleaching (GSB) signal at 561 nm is observed for BC in cyclohexane, as well as two weak absorption bands in 400–480 nm and 650–800 nm (Fig. 4a). These absorption peaks disappear in the air-saturated solutions (Fig. S4), indicating that these transient absorptions are contributed by triplet excited states. Compared with the reported data of BDP monomer [31], these peaks belong to the characteristic transient absorptions of the triplet BDP. The similar transient absorption spectra are observed in toluene and dichloroethane solvents (in Fig. 4b and c). Therefore, the triplet BDP unit is produced in BC dyad due to ISC with photoexcitation at 532 nm, which is greatly consistent with the calculated spin density distributions. In addition, although the peak positions do not show visible changes, the absorption intensities are highly dependent on the solvent polarity, i.e. the peak intensity is reduced with the increase of solvent polarity.

Table 1
Photophysical properties of BC and CBC^a.

Sample	Solvent ^b	λ_{abs} ^c	ϵ^d	λ_{em} ^e	Φ_F ^f	Φ_T ^g	Φ_{Δ} ^h	τ_T ⁱ
BC	Cyclohexane (2.05)	553	4.46	610	16.0	4.5	2.7	9.6
	Toluene (2.24)	553	4.29	618	11.0	3.9	3.8	75.6
	Dichloroethane (10.5)	552	4.30	630	2.3	1.8	2.1	204.7
CBC	Cyclohexane (2.05)	599	3.28	637	18.4	9.1	6.9	118.2
	Toluene (2.24)	598	3.12	645	14.0	7.9	8.2	175.7
	Dichloroethane (10.5)	595	3.07	655	2.2	3.7	3.4	464.7

^a $c[\text{photosensitizer}] = 1.0 \times 10^{-5}$ M.

^b The values in parentheses are the dielectric constants of solvents.

^c Absorption peak position, nm.

^d Molar extinction coefficient at the maximal absorption, $10^4 \text{ M}^{-1} \text{ cm}^{-1}$.

^e Fluorescence emission peak position, nm.

^f Fluorescence quantum yield, 2I-BDP as the standard ($\Phi_F = 2.7$ % in ACN), %.

^g Triplet state quantum yield, 2I-BDP as the standard ($\Phi_T = 88$ % in Toluene), %.

^h The Quantum yield of singlet oxygen ($^1\text{O}_2^*$), 2I-BDP as standard ($\Phi_{\Delta} = 83$ % in Toluene), %.

ⁱ Triplet lifetime, μs .

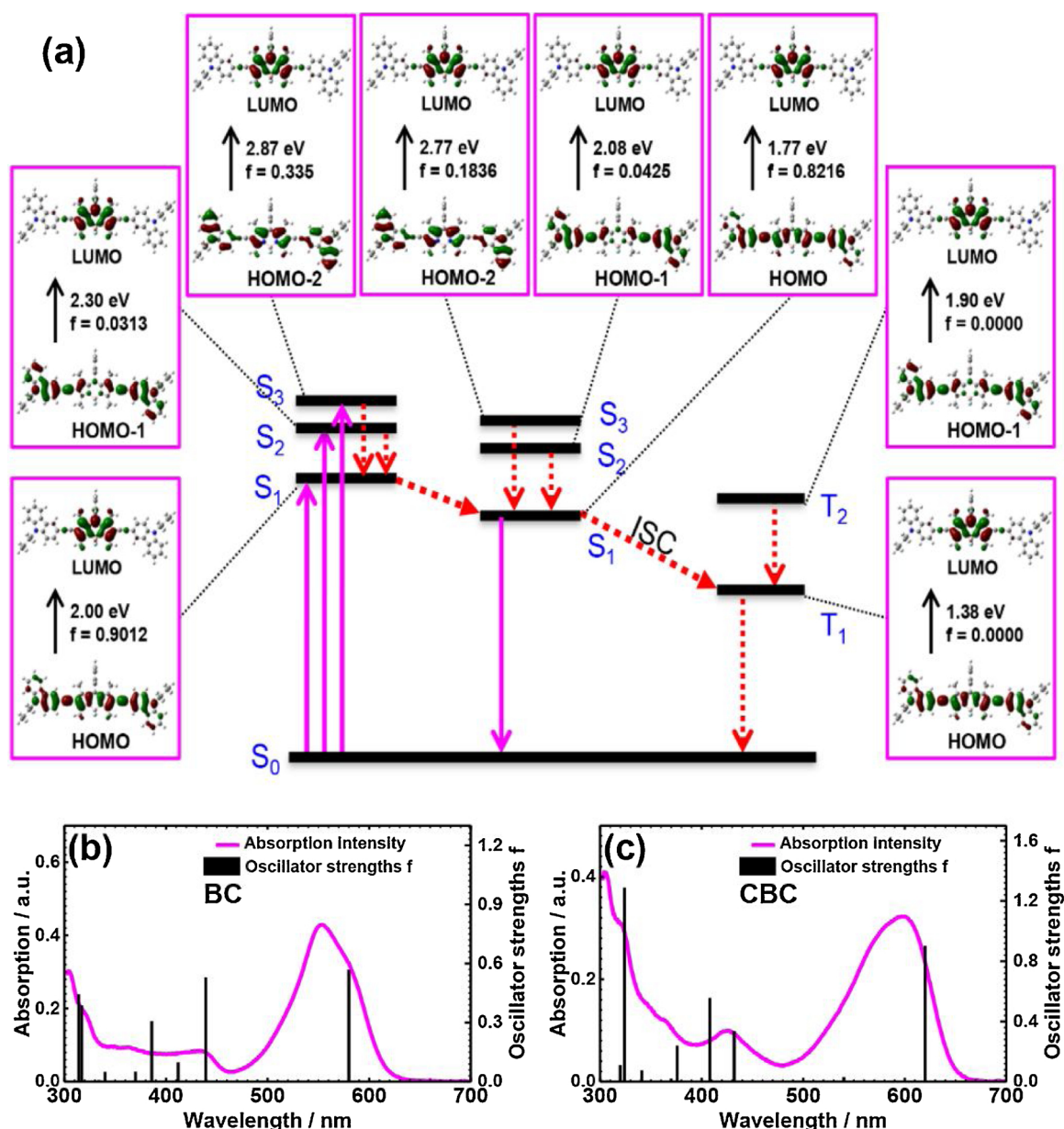


Fig. 2. (a) Frontier molecular orbitals involved in the singlet and triplet excited states of CBC; (b) The experimental absorption spectra (solid lines) and the calculated Franck-Condon transitions (sticks) of BC; (c) The experimental spectra and the calculated transitions of CBC. The calculations were performed at the B3LYP/6-31 G(d) level using toluene as the solvent.

Similar results were observed for CBC (Fig. 4d-4f), with a strong GSB located at 600 nm. In addition, the transient absorption spectrum of the BDP monomer was also measured as plotted in Fig. S5 of ESI, however, no transient absorption band was clearly found, indicative of no production of the triplet BDP monomer.

Through analyzing the depletion of GSB peak (Fig. 5), the triplet state quantum yields (Φ_T) can be calculated for BC and CBC in different solvents as described in the ESI. As shown in Table 1, these Φ_T values are dramatically decreased with the solvent polarity, for instance, for BC 4.5 % in cyclohexane, 3.9 % in toluene, and 1.8 % in dichloroethane. While the triplet quantum yields of CBC were determined as 9.1 % in cyclohexane, 7.9 % in toluene, and 3.7 % in dichloroethane. According to the previous conclusions of the SOCT-ISC mechanism [25,32], the triplet state quantum yield is usually very low in nonpolar solvents, while it increases in polar solvents. Our experimental results are on the contrary, reminding us a different ISC mechanism for both BC and CBC. Actually, our DFT calculations also confirm that the SOCT-

ISC mechanism is impossible in BC and CBC dyads due to their unsuitable planar configurations. Instead, the intramolecular charge transfer is feasible to occur when the photosensitizers are photoexcited, as suggested by the spin density and frontier molecular orbital calculations. Thus, the triplet state in the BC and CBC dyads might be produced via the intramolecular charge transfer and recombination, instead of direct ISC of the BDP unit. It is known that the ISC rate of the BDP unit itself is increased with the solvent polarity [31]. Following the direct ISC mechanism, the Φ_T values of dyads should be increased with the solvent polarity, which is obviously opposite to the present experimental conclusion. Hence, the intramolecular charge transfer and recombination becomes the unique ISC mechanism for BC and CBC. Owing to the larger dipole moment of the excited state compared with that of the ground state, the charge separation state can be efficiently stabilized in polar solvents to reduce the possibility of charge recombination. As a result, the Φ_T s of the dyads decrease with the solvent polarity, as indicated in Table 1. According to the ultrafast charge

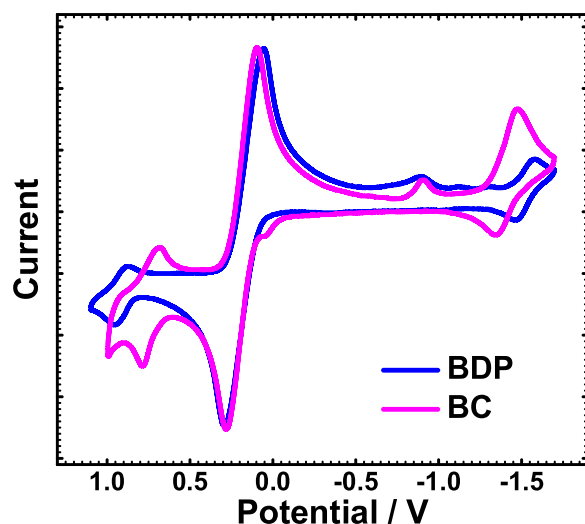


Fig. 3. Cyclic voltammograms of BDP monomer and BC in deaerated dichloroethane solution at 25 °C, where ferrocene (Fc) and Ag/AgNO₃ reference electrodes were used, with 0.1 M Bu₄NPF₆ as the supporting electrolyte. The scan rate was 50 mV/s.

separation and recombination, the absorption of these intermediates did not be observed in our experiments, but the femtosecond time-resolved transient absorption spectroscopy can verify this mechanism in experiment.

By fitting the decay kinetic curves in Fig. 5a, the lifetime of triplet BC is determined to be 9.6 μs in cyclohexane, and it is markedly improved to 204.7 μs in dichloroethane. In fact, similar to the S₁ state, the dipole moment (μ_T) of the triplet state is also larger than that of the ground state (μ_g), resulting in that it can be significantly stabilized in polarity solvents. Similar phenomena were observed for CBC (Fig. 5b). As indicated in Table 1, the lifetime of triplet CBC increases from 118.2 μs in cyclohexane to 464.7 μs in dichloroethane. In summary, the more efficient stabilization of triplet states in polar solvents prolongs their lifetimes.

3.4. Photo-oxidation of DHN with BC and CBC as triplet photosensitizers

Based on the long lifetimes, the triplet photosensitizers can efficiently sensitize ¹O₂ [33,34]. Some BDP-fullerene complexes as organic photosensitizers were reported to sensitize oxygen [33,35] as the environmental friendly and less biological toxic photosensitizers to replace those containing heavy metal atoms [1,36]. Herein, these two new organic photosensitizers, BC and CBC, were applied in photooxidation of DHN, where the well-known product is juglone [8] as shown in Fig. 6a.

As previously reported [8,37,38], the concentration of juglone as the oxidation product of DHN was usually determined by analyzing its characteristic absorption intensity at 427 nm ($\epsilon = 3811 \text{ M}^{-1} \text{ cm}^{-1}$). The quantum yield of juglone is determined by dividing its concentration with the initial concentration of DHN. Although this peak is slightly overlapped with the absorption of BC and CBC, the observed peak is believed to be mainly contributed by juglone and DHN according to the large different concentrations between them and photosensitizers. Fig. 6b shows the time-dependent absorption spectra of DHN and CBC under photoexcitation of visible light, as an example. With the delay of irradiation time, the consumption of DHN can be monitored by the reduction of the absorption intensity at 301 nm ($\epsilon = 7664 \text{ M}^{-1} \text{ cm}^{-1}$), while the absorption at 427 nm is significantly enhanced, indicative of the production of juglone. Similar results were observed with BC as the triplet photosensitizer (ESI, Fig. S11). For comparison, the time-dependent absorption spectrum of DHN under visible photoexcitation with the absence of photosensitizers was also measured (Fig. S10), where the absorption intensity at 301 nm as the absorption of DHN was almost unchanged.

In photo-oxidation of DHN using triplet photosensitizers, the reaction rate k_{obs} was determined by fitting the consumption of DHN over the reaction time with the Eq. (1), using the pseudo first order reaction approximation [1,37].

$$\ln(C_t/C_0) = -k_{\text{obs}} t \quad (1)$$

Where C_0 and C_t are the concentrations of DHN at the initial ($t = 0$) and a certain time. Fig. 6c shows the dependent curves of $\ln(C_t/C_0)$ vs t . As listed in Table 2, the photoreaction rate constants, k_{obs} , are determined as $1.11 \times 10^{-3} \text{ min}^{-1}$ for BC and $2.54 \times 10^{-3} \text{ min}^{-1}$ for CBC, respectively.

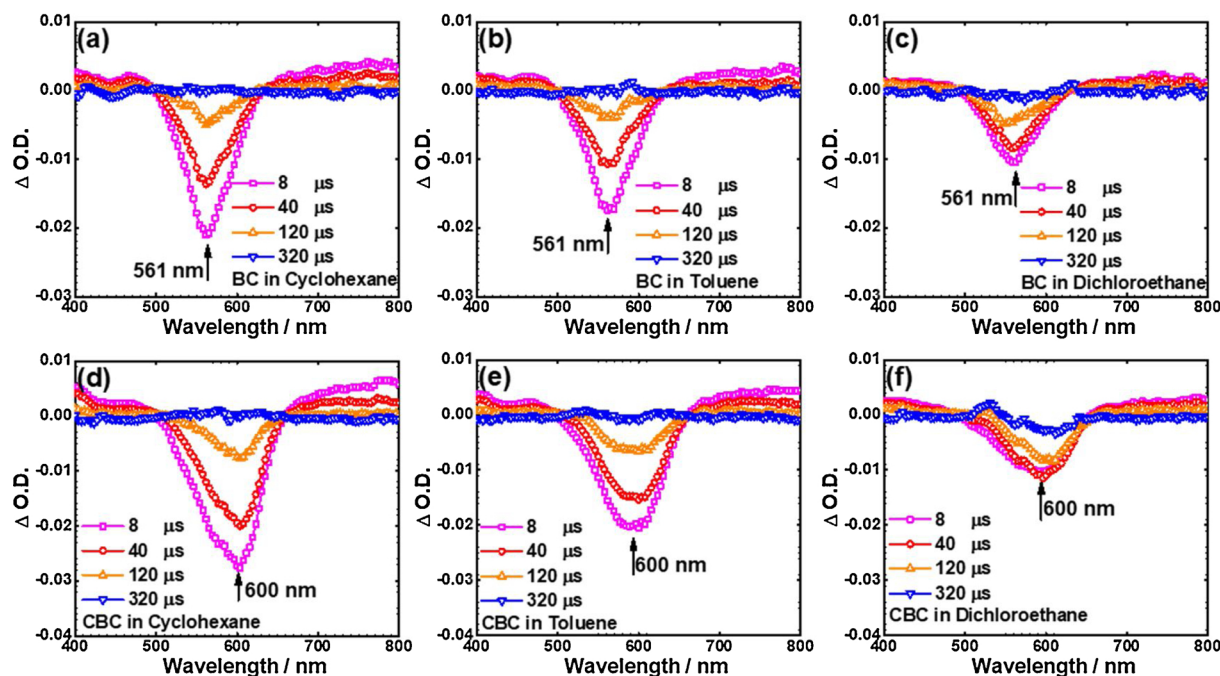


Fig. 4. Nanosecond transient absorption spectra at 25 °C of BC (the upper curves) and CBC (the lower traces) in the deoxygenated cyclohexane (a,d), toluene (b,e), and dichloroethane (c,f), respectively, where the concentration of photosensitizer is $2 \times 10^{-5} \text{ M}$.

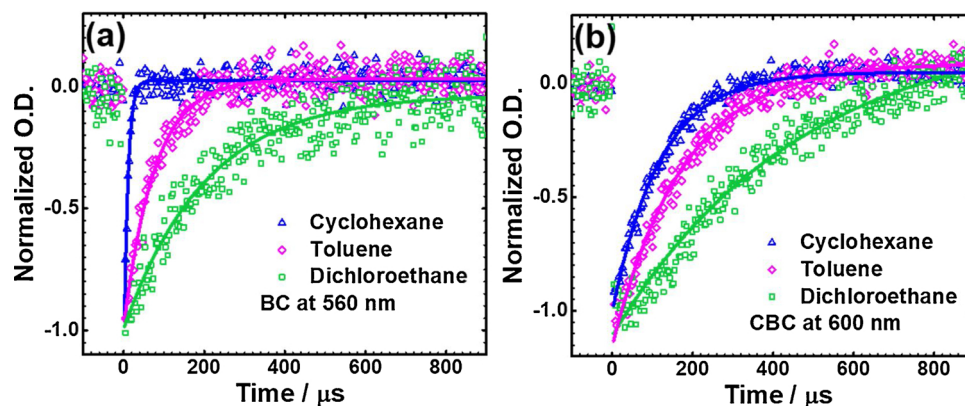


Fig. 5. The decay kinetic curves (at 25°C) of the GSB peaks of BC (a) and CBC (b) in deoxygenated cyclohexane, toluene, and dichloroethane, where the concentration of photosensitizer was 2×10^{-5} M.

As shown in photo-oxidation mechanism of DHN with triplet photosensitizers (Fig. 6a), the quantum yield of $^1\text{O}_2$ is crucial to assess the effects of photosensitizers. Thus, an additional experiment was performed to accurately measure the quantum yield of $^1\text{O}_2$ with 1,3-diphenylisobenzofuran (DBPF), which was widely used as the $^1\text{O}_2$ scavenger. Photosensitizers, BC, CBC and 2I-BDP, were excited at 545 nm in different solvents, where the 2I-BDP as the reference. As shown in Fig. S8, the absorption of mix solution (photosensitizer and DBPF) at 414 nm is decreased with the extension of photoirradiation time, while the blank reference (only DBPF) is almost unchanged (Fig. S9). The quantum yields of $^1\text{O}_2$ were determined to be 3.8 % for BC in toluene, 8.2 % for CBC in toluene (Table 1). After irradiation for 28 min at a light power density of 40 mW cm^{-2} , the yield of juglone produced by photooxidation of DHN was 5.3 % for BC and 15.7 % for CBC. Apparently, CBC is more efficient to sensitize $^1\text{O}_2$ than BC, which is consistent with their triplet state quantum yields (Table 1).

Table 2

Photo-oxidation rate constants of DHN.

Photosensitizers	k_{obs} (10^{-3} min^{-1})	η^a (%)
BC	1.11	5.3
CBC	2.54	15.7

^a Yield of juglone produced by photooxidation of DHN, $t = 28$ min, light power density of 40 mW cm^{-2} .

4. Conclusions

In summary, two new metal-free photosensitizers of BDP derivatives, BC and CBC, were synthesized and applied for the photo-oxidation of DHN. Both triplet BC and CBC are found to have the triplet BDP unit, which are produced by the intramolecular charge transfer in the Franck-Condon excitation. The triplet state quantum yields of BC and

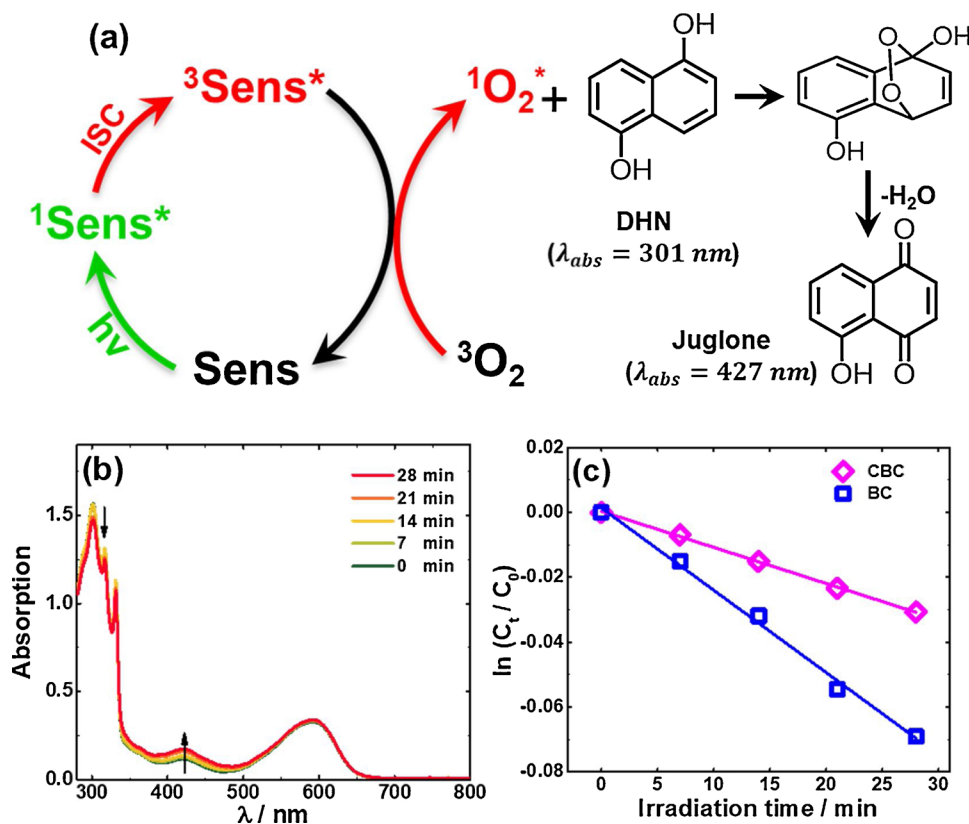


Fig. 6. (a) The photo-oxidation mechanism of DHN with triplet photosensitizers; (b) The time-dependent absorption spectra (at 25°C) of DHN (1×10^{-4} M) in $\text{CH}_2\text{Cl}_2/\text{MeOH}$ (9:1, v/v), with CBC as the triplet photosensitizer (1×10^{-5} M) under light power density of 40 mW cm^{-2} ; (c) The logarithmic plot of the C_t/C_0 ratio at 427 nm as a function of the irradiation time t .

CBC are determined to be 4.5 % and 9.1 % in cyclohexane, and decrease to 1.8 % and 3.7 % in dichloroethane. Meanwhile, their triplet lifetimes also show a dependence on the solvent polarity, e.g. 9.6 and 118.2 μs in cyclohexane, while, 204.7 and 464.7 μs in dichloroethane for BC and CBC, respectively. With the aid of DFT calculations, the dependent behavior of photophysical properties of these triplet photosensitizers on the solvent polarity is associated with the charge transfer and the stabilization of polar solvent. Moreover, the photo-oxidation rate constants of DHN with BC and CBC as triplet photosensitizers are determined to be $1.11 \times 10^{-3} \text{ min}^{-1}$ and $2.54 \times 10^{-3} \text{ min}^{-1}$ for BC and CBC, respectively.

CRedit authorship contribution statement

Yuanming Li: Investigation, Visualization, Formal analysis. **Yaxiong Wei:** Conceptualization, Methodology, Writing - original draft. **Xiaoguo Zhou:** Conceptualization, Resources, Writing - review & editing, Project administration, Funding acquisition.

Declaration of Competing Interest

The authors declare that they have no known competing financial interests or personal relationships that could have appeared to influence the work reported in this paper.

Acknowledgment

This work was supported by the National Natural Science Foundation of China (Grant Nos. 21873089 and 21573210). The quantum chemical calculations in this study were performed on the supercomputing system in the Supercomputing Center of the University of Science and Technology of China.

Appendix A. Supplementary data

Supplementary material related to this article can be found, in the online version, at doi:<https://doi.org/10.1016/j.jphotochem.2020.112713>.

References

- [1] S.-Y. Takizawa, R. Aboshi, S. Murata, Photooxidation of 1,5-dihydroxynaphthalene with iridium complexes as singlet oxygen sensitizers, *Photochem. Photobiol. Sci.* 10 (2011) 895–903.
- [2] J.W. Tucker, C.R. Stephenson, Shining light on photoredox catalysis: theory and synthetic applications, *J. Org. Chem.* 77 (2012) 1617–1622.
- [3] X.Z. Wang, Q.Y. Meng, J.J. Zhong, X.W. Gao, T. Lei, L.M. Zhao, Z.J. Li, B. Chen, C.H. Tung, L.Z. Wu, The singlet excited state of BODIPY promoted aerobic cross-dehydrogenative-coupling reactions under visible light, *Chem. Commun.* 51 (2015) 11256–11259.
- [4] Q. Zhou, Y. Wei, X. Liu, L. Chen, X. Zhou, S. Liu, Photochemical reaction between 1,2-naphthoquinone and adenine in binary water-acetonitrile solutions, *Photochem. Photobiol.* 48 (2017) 2467–2478.
- [5] S.O. McDonnell, M.J. Hall, L.T. Allen, A. Byrne, W.M. Gallagher, D.F. O'Shea, Supramolecular photonic therapeutic agents, *J. Am. Chem. Soc.* 127 (2005) 16360–16361.
- [6] C. Göl, M. Malkoç, S. Yeşilot, M. Durmuş, Novel zinc(II) phthalocyanine conjugates bearing different numbers of BODIPY and iodine groups as substituents on the periphery, *Dyes Pigm.* 111 (2014) 81–90.
- [7] Y. Wei, M. Zhou, Q. Zhou, X. Zhou, S. Liu, S. Zhang, B. Zhang, Triplet-triplet annihilation upconversion kinetics of C60-Bodipy dyads as organic triplet photosensitizers, *Phys. Chem. Chem. Phys.* 19 (2017) 22049–22060.
- [8] C. Zhang, J. Zhao, S. Wu, Z. Wang, W. Wu, J. Ma, S. Guo, L. Huang, Intramolecular RET enhanced visible light-absorbing bodipy organic triplet photosensitizers and application in photooxidation and triplet-triplet annihilation upconversion, *J. Am. Chem. Soc.* 135 (2013) 10566–10578.
- [9] K.A. El Roz, F.N. Castellano, Photochemical upconversion in water, *Chem. Commun.* 53 (2017) 11705–11708.
- [10] Y.Q. Zou, L.Q. Lu, L. Fu, N.J. Chang, J. Rong, J.R. Chen, W.J. Xiao, Visible-light-induced oxidation/[3+2] Cycloaddition/Oxidative aromatization sequence: a photocatalytic strategy to construct pyrrole [2, 1-a] isoquinolines, *Angew. Chem. Int. Ed.* 50 (2011) 7171–7175.
- [11] W. Wu, L. Liu, X. Cui, C. Zhang, J. Zhao, Red-light-absorbing diimine Pt(II) bisacetylidyde complexes showing near-IR phosphorescence and long-lived ^3IL excited state of Bodipy for application in triplet-triplet annihilation upconversion, *Dalton Trans.* 42 (2013) 14374–14379.
- [12] X. Yang, X. Wu, D. Zhou, J. Yu, G. Xie, D.W. Bruce, Y. Wang, Platinum-based metallomesogens bearing a Pt(4,6-dfppy)(acac) skeleton: synthesis, photophysical properties and polarised phosphorescence application, *Dalton Trans.* 47 (2018) 13368–13377.
- [13] X. Wu, D.G. Chen, D. Liu, S.H. Liu, S.W. Shen, C.I. Wu, G. Xie, J. Zhou, Z.X. Huang, C.Y. Huang, S.J. Su, W. Zhu, P.T. Chou, Highly emissive dinuclear platinum(III) complexes, *J. Am. Chem. Soc.* 142 (2020) 7469–7479.
- [14] S. Balushev, V. Yakutkin, T. Miteva, Y. Avlasevich, S. Chernov, S. Aleshchenkov, G. Nelles, A. Cheprakov, A. Yasuda, K. Mullen, G. Wegner, Blue-green up-conversion: noncoherent excitation by NIR light, *Angew. Chem. Int. Ed.* 46 (2007) 7693–7696.
- [15] B. Wang, B. Sun, X. Wang, C. Ye, P. Ding, Z. Liang, Z. Chen, X. Tao, L. Wu, Efficient triplet sensitizers of palladium(II) tetraphenylporphyrins for upconversion-powered photoelectrochemistry, *J. Phys. Chem. C* 118 (2014) 1417–1425.
- [16] J. Yu, H. Tan, F. Meng, K. Lv, W. Zhu, S. Su, Benzotriazole-containing donor-acceptor-acceptor type cyclometalated iridium(III) complex for solution-processed near-infrared polymer light emitting diodes, *Dyes Pigm.* 131 (2016) 231–238.
- [17] Y. Wei, M. Zheng, L. Chen, X. Zhou, S. Liu, Near-infrared to violet triplet-triplet annihilation fluorescence upconversion of Os(II) complexes by strong spin-forbidden transition, *Dalton Trans.* 48 (2019) 11763–11771.
- [18] Y. Wei, Y. Li, M. Zheng, X. Zhou, Y. Zou, C. Yang, Simultaneously high upconversion efficiency and large anti-stokes shift by using Os(II) complex dyad as triplet photosensitizer, *Adv. Opt. Mater.* 8 (2020) 1902157.
- [19] J. Zhao, S. Ji, W. Wu, W. Wu, H. Guo, J. Sun, H. Sun, Y. Liu, Q. Li, L. Huang, Transition metal complexes with strong absorption of visible light and long-lived triplet excited states: from molecular design to applications, *RSC Adv.* 2 (2012) 1712–1728.
- [20] W. Xiong, F. Meng, C. You, P. Wang, J. Yu, X. Wu, Y. Pei, W. Zhu, Y. Wang, S. Su, Molecular isomeric engineering of naphthyl-quinoline-containing dinuclear platinum complexes to tune emission from deep red to near infrared, *J. Mater. Chem. C* 7 (2019) 630–638.
- [21] J. Zhao, K. Chen, Y. Hou, Y. Che, L. Liu, D. Jia, Recent progress in heavy atom-free organic compounds showing unexpected intersystem crossing (ISC) ability, *Org. Biomol. Chem.* 16 (2018) 3692–3701.
- [22] T.N. Singhrachford, F.N. Castellano, Low power visible-to-UV upconversion, *J. Phys. Chem. A* 113 (2009) 5912–5917.
- [23] N. Yanai, M. Kozue, S. Amemori, R. Kabe, C. Adachi, N. Kimizuka, Increased vis-to-UV upconversion performance by energy level matching between a TADF donor and high triplet energy acceptors, *J. Mater. Chem. C* 4 (2016) 6447–6451.
- [24] Y. Wei, M. Zheng, Q. Zhou, X. Zhou, S. Liu, Application of a bodipy-C₇₀ dyad in triplet-triplet annihilation upconversion of perylene as a metal-free photosensitizer, *Org. Biomol. Chem.* 16 (2018) 5598–5608.
- [25] Z. Wang, J. Zhao, Bodipy-anthracene Dyads as triplet photosensitizers: effect of chromophore orientation on triplet-state formation efficiency and application in triplet-Triplet annihilation upconversion, *Org. Lett.* 19 (2017) 4492–4495.
- [26] K. Chen, W. Yang, Z. Wang, A. Iagatti, L. Bussotti, P. Foggi, W. Ji, J. Zhao, M. Di Donato, Triplet excited state of BODIPY accessed by charge recombination and its application in triplet-triplet annihilation upconversion, *J. Phys. Chem. A* 121 (2017) 7550–7564.
- [27] P. Yang, W. Wu, J. Zhao, D. Huang, X. Yi, Using C₆₀-bodipy dyads that show strong absorption of visible light and long-lived triplet excited states as organic triplet photosensitizers for triplet-triplet annihilation upconversion, *J. Mater. Chem.* 22 (2012) 20273–20283.
- [28] M. Frisch, G. Trucks, H.B. Schlegel, G. Scuseria, M. Robb, J. Cheeseman, G. Scalmani, V. Barone, B. Mennucci, G. Petersson, Gaussian 09, Revision a. 02, Gaussian, Inc., Wallingford, CT, 2009 200.
- [29] J.J. Cavaleri, K. Prater, R.M. Bowman, An investigation of the solvent dependence on the ultrafast intersystem crossing kinetics of xanthone, *Chem. Phys. Lett.* 259 (1996) 495–502.
- [30] C. Reichardt, T. Welton, Solvents and Solvent Effects in Organic Chemistry, John Wiley & Sons, 2011.
- [31] Q. Zhou, M. Zhou, Y. Wei, X. Zhou, S. Liu, S. Zhang, B. Zhang, Solvent effects on the triplet-triplet annihilation upconversion of diiodo-bodipy and perylene, *Phys. Chem. Chem. Phys.* 19 (2017) 1516–1525.
- [32] C.B. Kc, G.N. Lim, V.N. Nesterov, P.A. Karr, F. D'Souza, Phenothiazine-BODIPY-fullerene triads as photosynthetic reaction center models: substitution and solvent polarity effects on photoinduced charge separation and recombination, *Chem.-Eur. J.* 20 (2014) 17100–17112.
- [33] L. Huang, X. Cui, B. Therrien, J. Zhao, Energy-funneling-based broadband visible-light-absorbing bodipy-C₆₀ triads and tetrad as dual functional heavy-atom-free organic triplet photosensitizers for photocatalytic organic reactions, *Chemistry* 19 (2013) 17472–17482.

- [34] T. Yogo, Y. Urano, Y. Ishitsuka, F. Maniwa, T. Nagano, Highly efficient and photostable photosensitizer based on BODIPY chromophore, *J. Am. Chem. Soc.* 127 (2005) 12162–12163.
- [35] L. Huang, X. Yu, W. Wu, J. Zhao, Styryl Bodipy-C60 dyads as efficient heavy-atom-free organic triplet photosensitizers, *Org. Lett.* 14 (2012) 2594–2597.
- [36] Y.Q. Zou, J.R. Chen, X.P. Liu, L.Q. Lu, R.L. Davis, K.A. Jorgensen, W.J. Xiao, Highly efficient aerobic oxidative hydroxylation of arylboronic acids: photoredox catalysis using visible light, *Angew. Chem. Int. Ed.* 51 (2012) 784–788.
- [37] Q.-J. Hu, Y.-C. Lu, C.-X. Yang, X.-P. Yan, Synthesis of covalently bonded boron-dipyrromethene–diarylethene for building a stable photosensitizer with photo-controlled reversibility, *Chem. Commun.* 52 (2016) 5470–5473.
- [38] S. Guo, L. Ma, J. Zhao, B. Küçüköz, A. Karatay, M. Hayvali, H.G. Yaglioglu, A. Elmali, BODIPY triads triplet photosensitizers enhanced with intramolecular resonance energy transfer (RET): broadband visible light absorption and application in photooxidation, *Chem. Sci.* 5 (2014) 489–500.